Polym. Korea, Vol. 50, No. 5, pp. 687-696 (2026)
https://doi.org/10.7317/pk.2026.50.5.687
ISSN 2234-8077(Online)

서로 다른 금속 양이온에 의한 양이온-π 상호작용이 에폭시 수지의 기계적 물성에 미치는 영향

Heshuang Li#, Sijie Yin#, Jingya Liu*, Qiaolin Tang, Qiang Peng, Ai Lu**,
Yunbo Xu***, JingJin Huang****, and Ming Kang†
School of Material and Chemistry, State Key Laboratory of Environment-friendly Energy Materials,
Southwest University of Science and Technology
*Zigong Centre for Disease Control and Prevention, Institute of Physical and Chemical
**National Key Laboratory of Chemical Explosion Safety, Institute of Chemical Materials,
China Academy of Engineering Physics
***Sichuan Shutai Chemical Technology Co., Ltd.
****Sichuan Coremer Materials Co., Ltd.
(2026년 3월 27일 접수, 2026년 5월 24일 수정, 2026년 6월 3일 채택)

Research on the Influence of Cation-π Interactions Formed by Different Metal Cations on the Mechanical Properties of Epoxy Resin

Heshuang Li#, Sijie Yin#, Jingya Liu*, Qiaolin Tang, Qiang Peng, Ai Lu,
Yunbo Xu***, JingJin Huang****, and Ming Kang†**
*School of Material and Chemistry, State Key Laboratory of Environment-friendly Energy Materials,
Southwest University of Science and Technology, Mianyang 621010, P.R. China*
**Zigong Centre for Disease Control and Prevention, Institute of Physical and Chemical, Zigong 643000, P.R. China*
***National Key Laboratory of Chemical Explosion Safety, Institute of Chemical Materials,
China Academy of Engineering Physics, Mianyang, 621900, China*
****Sichuan Shutai Chemical Technology Co., Ltd, Suining 629399, P.R. China*
*****Sichuan Coremer Materials Co., Ltd., Mianyang 621010, P.R. China*
(Received March 27, 2026; Revised May 25, 2026; Accepted June 3, 2026)

Abstract: The polymerization of epoxy resin E44 with tryptamine was performed, and cation-π interaction-containing indole epoxy resins were prepared by doping with Na^+, Mg^{2+}, and K^+, respectively. A structure-property relationship study was conducted. The results indicated that when the IEP to Mg^{2+} doping ratio was 30:1, the modified epoxy resin exhibited optimal mechanical properties, with a tensile strength of 62.88 MPa and a fracture elongation of 9.52%. The cation-π interactions constructed by introducing Na^+, Mg^{2+}, and K^+ can simultaneously enhance and toughen the material, and significant differences exist in the enhancement and toughening effects of the three cations. There is a certain correlation between the macroscopic enhancement effect and both the cation-π interactions and the intrinsic parameters of the ions.

Keywords: cations-π interaction, epoxy resin, mechanical properties, weak interaction.

Introduction

Cation-π interaction, as a weak non-covalent force, distinguishes itself from traditional interactions like hydrogen bonds and ion pairs through electrostatic attraction between cations and π-electron systems.[1,2] This unique interaction has emerged as a critical non-covalent binding mechanism that influences molecular structure and function, garnering extensive attention in fields such as chemistry and biology.[3,4] Cation-π interactions play a role in material properties, molecular recognition and assembly, luminescent material in materials science and chemistry.[5-7] Through the multiple cross-linking of the polymer network and the cation-π interactions of PIL chains, a tough and impact-resistant poly(ionic liquid)/poly(2-hydroxyethyl acry-

#These authors contributed equally to this manuscript.
†To whom correspondence should be addressed.
dyw510@126.com, ORCID 0000-0001-7189-7466

late) double-network elastomer was constructed.[8] Peptide-based amphiphiles with cation-π interaction pairs can self-assemble into supramolecular hydrogels under physiological conditions. The study investigated their effects on the peptide folding tendency, morphology and rigidity of the resulting hydrogels.[9] In the biomedical field, cation-π interactions play a role in biofouling prevention and control. The synthesized copolymer can rapidly form a fouling-resistant coating on metal-phenolic network-modified substrates based on cation-π interactions, effectively resisting proteins, cells, and bacteria.[10] Regarding environmental protection, by integrating click chemistry with cation-π interactions, He has synthesized high-performance epoxy resin materials with recyclability and processability.[11]

Cation-π interactions are also widely utilized to enhance or modify polymer properties.[12] In terms of mechanical properties, a cation-π cross-linked polyimide (sodium poly(arylindole)imide, Na-PINI) film with strong mechanical performance and heat resistance was constructed.[13] In terms of fluorescent properties, the mechanical performance and wide-color-gamut chromaticity tunability of the polymer are improved through rare-earth cation-π interactions.[14] In terms of thermal performance, the cross-linked structure formed by cation-π interactions enhances the glass transition temperature and thermal insulation properties of polyimide foam.[15] In marine antifouling research, a novel silicone material was developed by leveraging the interaction between cations and indole derivatives. This material effectively shields ultraviolet light and inhibits the growth of *Escherichia coli* and *Staphylococcus aureus*.[16]

The influence of metal cation-π interactions on polymers has been extensively studied by researchers.[17] However, there is rarely reported analysis on how cation-π interactions affect the structure-property relationships in polymers. This study will investigate the structure-property relationships of Indole based epoxy resin by examining the effects of cation-π interactions formed with different metal cations (Na^+, Mg^{2+} and K^+) on their mechanical properties. Indole-containing epoxy resins (IEP) will be synthesized, and metal cations will be introduced to form high-energy indole-metal cation-indole cation-π dynamic crosslinking networks between molecular chains (similar to sandwich structure). The mechanical and thermal properties of indole-containing epoxy resins were enhanced by cation-π interaction, and visualized using Interaction Region Indicator Functions (IRI).[18] It has been demonstrated that the cation-π interaction formed by three types of cations can enhance and toughen epoxy resin, and a comparative analysis has been conducted on the enhancement and toughening effects of cation-π interactions formed by different cations. This study aims to provide more comprehensive data support for research on the mechanical properties of indole-containing epoxy resins based on cation-π interactions.

Experimental

Materials. Tryptamine (Try, AR, Macklin Biochemical, Shanghai), Bisphenol A-type epoxy resin E44 (98%, Macklin Biochemical, Shanghai), *N*,*N*-dimethylformamide (DMF, AR, Kelong

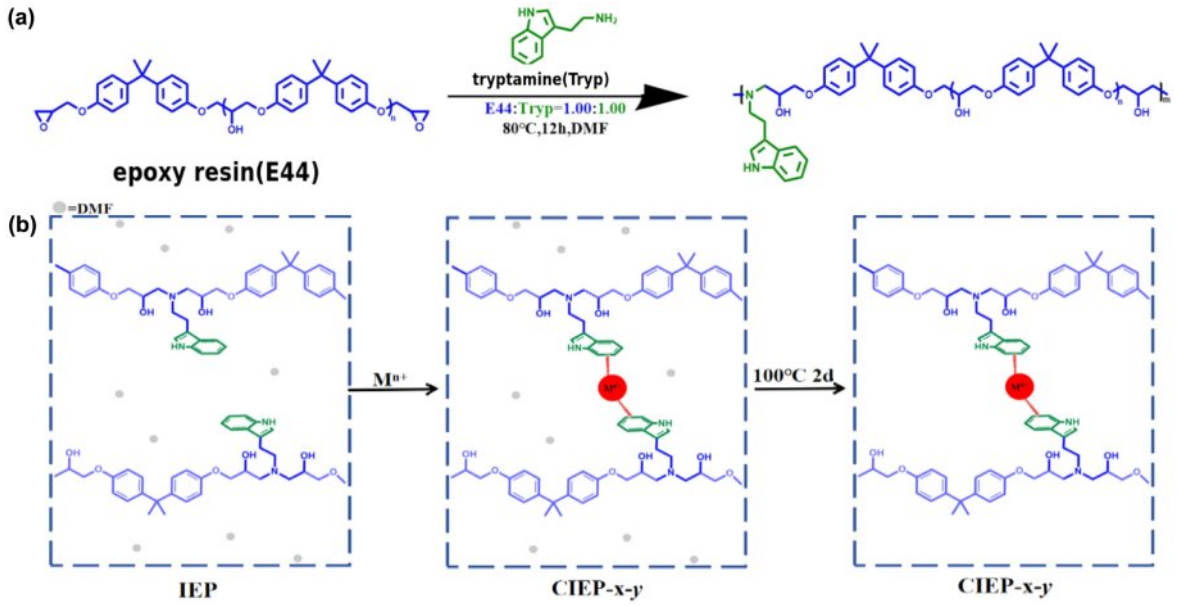

Figure 1. (a) Preparation of indole epoxy resin; (b) preparation of metal cation reinforced indole epoxy resin film.

Reagent, Chengdu), NaI, KI and $MgCl_2$ (AR, Xiya Reagent). Unless otherwise specified, all chemicals were purchased commercially and used as received without further purification.

All relevant information regarding the testing instruments can be found in the supporting materials.

The Preparation of Indole-containing Epoxy Resins. The preparation process of indole-containing epoxy resins (hereinafter referred to as IEP) is shown in Figure 1(a). Tryptamine (Try 16 g, 0.1 mol) was placed in a beaker, and DMF (20 mL) was added. The mixture was dissolved *via* oscillation in an ultrasonic cleaner. E44-type epoxy resin (45.5 g, 0.1 mol) was placed in a three-necked flask, to which 20 mL of DMF and the dissolved tryptamine solution were added. The mixture was mechanically stirred under reflux at 80 °C in an oil bath for 12 h to obtain the IEP solution, and its solid content was calculated. The IEP solution was transferred to a silicone mold, placed in an electric hot-air oven at 100 °C for drying, and cooled and demolded to obtain the IEP film.

The Preparation of Metal Cation Indole-containing Epoxy Resin Film. The indole epoxy resin doped with metal cations is denoted as CIEP-x-y, where x represents the type of doped cation and y indicates the molar ratio of added cations. For example, when $y = 30$, the ratio of IEP: Mg^{2+} is 30 : 1. The preparation process is shown in Figure 1(b). A certain amount of IEP was taken, and the mass of the required cationic compound was calculated according to the ratio to meet the desired proportion. Subsequently, 5 mL of DMF was added to the cationic compound, which was then placed in an ultrasonic cleaner for dissolution. The obtained IEP was placed in a single-neck flask, the cation-containing solution was added. Mechanical stirring was performed at a speed of 280 rpm to obtain the CIEP-x-y solution. The solution was transferred to a silicone mold and placed in an electric thermostatic blast drying oven at 100 °C. After cooling and demolding, the CIEP-x-y film was obtained.

Theoretical Simulation. Theoretical simulation of metal cation-π interactions based on quantum chemistry (QC) and molecular dynamics (MD).

The structural design and theoretical calculations of quantum chemistry (QC) were performed using Gaussian software to demonstrate the existence of cation-π interactions.[19] The Berny algorithm was employed to locate stationary points by varying the distance between the cation and the indole plane, generating different conformations.

Density functional theory (DFT) calculations were initially carried out using the B3LYP/6-31G (d, p) method for geometry optimization, followed by energy refinement using the M06-2X functional and 6-311G (2d, p) basis set. After calculating the energies of cation-π interactions at different distances between metal cations and indole, scatter plots were generated. Differential analysis of these plots yielded scatter diagrams illustrating how the interaction force between the cation and indole varies with distance.

The interaction region indicator (IRI) was analyzed and visualized using the Multiwfn wavefunction analysis program and the VMD quantum chemistry visualization software.[20,21] In the IRI visualization of cation-π interactions, the sign $(\lambda_2)\,\rho$ function was projected onto IRI isosurfaces with different colors to distinguish interaction types and strengths across regions. Green isosurfaces in IRI indicate weak interaction regions (*e.g.*, cation-π interactions) at $\rho = 0$. Blue regions represent strong attractive interactions, such as hydrogen bonds or halogen bonds. Fully blue isosurfaces indicate strong interactions, while electron densities ≥ 0.04 a.u. denote chemical bonding. Red regions signify strong repulsive interactions, indicative of steric hindrance.[22] Finally, all-atom molecular dynamics (MD) simulations were conducted to study the equilibrium conformations of cation-indole complexes using the amorphous cell module in Materials Studio (Accelrys Software Inc.) with the COMPASSII force field. The radial distribution function analyzed the relative distances between rare-earth cations and indole within surrounding IEP chain segments at the molecular level, confirming the existence of cation-π interactions.[23]

Results and Discussion

Theoretical Simulation. Using the aforementioned theoretical simulation method, theoretical data on the cation-π interactions induced by different metal cations were obtained. The CIEP theoretical calculations for different cation-doped materials (Na^+ and K^+) are presented in the Figure S1 and FigureS2. Taking the Mg^{2+}-π interaction as an example, Figure 2 presents the theoretical calculations of the Mg^{2+}-π interaction. In Figure 2(a), the IRI isosurface plot of the Mg^{2+}-π interaction illustrates a weak but evident interaction between Mg^{2+} and the indole ring (green region). The dipole moment of the Mg^{2+}-indole system is 0.88 D, with an interaction energy (ΔE) of 61.34 kJ mol^{-1}. In Figure 2(b) presents a scatter plot of the Interaction Region Indicator (IRI) versus sign $(\lambda_2)\,\rho$. Near the zero point on the x-axis, a distinct green peak (corresponding to the π-ring interaction pattern in the green region of Figure 2(a)) can be observed, indicating weak interactions between Mg^{2+} and

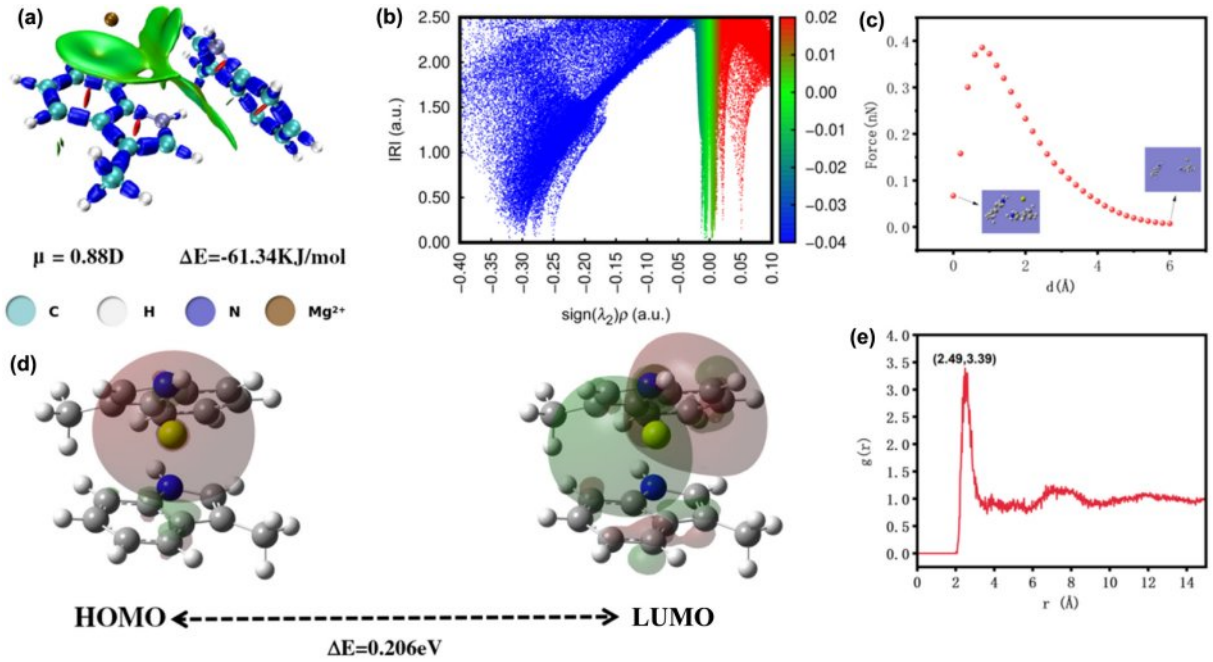

Figure 2. (a) IRI image of Mg^{2+} cation-π interaction; (b) IRI scatter plot; (c) the strength variation of cation-π interaction with the distance between Mg^{2+} and indole group; (d) cation-π interaction molecular orbital energy gap; (e) radial distribution function of distance between Mg^{2+} and indole.

indole. Figure 2(c) shows that when the distance between Mg^{2+} and indole is 0.8 Å, the maximum constraint force generated by their interaction is 0.386 nN. Figure 2(d) indicates that the energy difference between the HOMO and LUMO orbitals (ΔE) in the system is 0.206 eV, which is lower than the energy required for excitation without the Mg^{2+}-indole interaction, suggesting that electrons are more easily excited and undergo transitions. Figure 2(e) reveals that when the distance between Mg^{2+} and indole is 3.39 Å, the g(r) function reaches a maximum value of 2.49 > 1, indicating the presence of a weak interaction between Mg^{2+} and indole, i.e., the Mg^{2+}-π interaction.

The corresponding calculation figures for other metal cations are provided in the Supplementary Materials. According to the preliminary research conducted by our research group, in the pure IEP formed without the addition of cations in the epoxy resin, there exists an interfacial π-π interaction, with an interaction energy of -39.08 KJ/mol.[24] Table 1 presents the interaction energy of π-π interaction at the interface in indole epoxy resin and the interaction energies and maximum constraint forces between different cations and the indole moiety. As shown in the table, the interaction energies of these three cations follow the trend: Within the same group: $Na^+ < K^+$. Within the same period: $Na^+ > Mg^{2+}$. The maximum binding strengths of the four cations are as follows: Within the same group: $Na^+ \approx K^+$; Within the same period: $Na^+ > Mg^{2+}$. In summary, the order of interaction energy is: $Mg^{2+} < Na^+ < K^+$. For elements in the group, the difference in ionic radius has little effect on the interaction energy and maximum binding strength of cation-π interactions. For elements in the period, both charge and ionic radius differ, resulting in a effect that significantly influences the cation-π interaction.

Table 1. The Interaction Energy Between Different Cation-π Interactions and Indole, as Well as the Maximum Binding Force Between Cations and Indole

Sample	Interaction energy (kJ\mol)	Maximum constraint force (nN)
CIEP-Na^+	-80.90	0.554
CIEP-Mg^{2+}	-61.34	0.386
CIEP-K^+	-86.18	0.551
IEP(π-π)[24]	-39.08	\

Analysis of Synthesis Results of Epoxy Resin. Based on the experimental protocol, the IEP and CIEP-x-y were obtained. To verify that the doped cations form cross-linked structures *via* non-covalent interactions rather than covalent bonds, structural analysis was conducted. Initially, Fourier transform infrared spectroscopy (FTIR) was employed to characterize the synthesis results of E44, IEP and CIEP-x-y. In Figure 3(a), the absorption peak at 1243 cm^{-1} corresponds to the asymmetric stretching

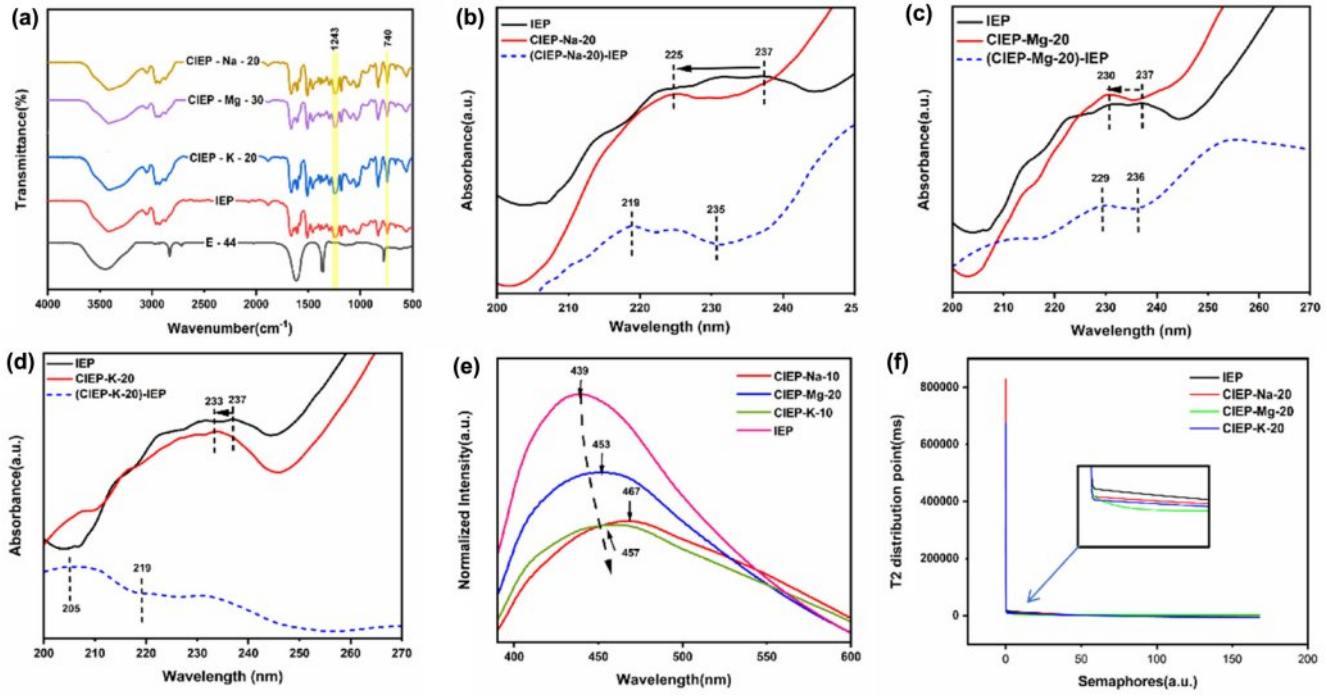

Figure 3. (a) Infrared spectra of IEP and CIEP-x-y; (b) UV spectra of IEP and CIEP-Na-20; (c) UV spectra of IEP and CIEP-Mg-30; (d) UV spectra of IEP and CIEP-K-20; (e) Fluorescence spectra of IEP and CIEP-x-y; (f) IEP and CIEP-x-y low-field solid-state NMR spectra.

vibration of C-O-C. Both IEP and CIEP-x-y exhibit this absorption peak, while E44 does not. The absorption peak at 740 cm^{-1} represents the out-of-plane bending vibration of the ortho-substituted aromatic ring, which is the characteristic infrared peak of tryptamine. E44 lacks the indole structure's characteristic infrared peak at 740 cm^{-1}, whereas both IEP and CIEP-x-y display this absorption peak. This indicates that Tryptamine is linked to E44 via covalent bonds to form a polymer. Compared to IEP, the peak profiles of the other CIEP-x-y samples are consistent with IEP, lacking additional absorption peaks. This suggests that cation addition occurs via non-covalent interactions rather than through covalent bonds.

Infrared spectroscopy supports this interpretation, cations undergo structural cross-linking through non-covalent bonds. To further clarify the role of cation-π in CIEP-x-y, UV visible absorption spectroscopy and fluorescence spectroscopy were performed on IEP and CIEP-x-y.

Using a ultraviolet-visible spectrophotometer, the ultraviolet-visible absorption spectra of IEP cross-linked with three different cations were obtained, as shown in Figure 3(b), 3(c) and 3(d). Compared to IEP, the π-π absorption peaks of the indole groups in CIEP-x-y all exhibit different degrees of blue shift, and the difference spectra show relatively obvious positive and negative bands at different wavelengths, indicating that the three different cations have formed stable cation-π interactions with the indole groups of IEP.[25] Using a fluorescence spectrophotometer, the fluorescence spectra of IEP and CIEP-x-y were obtained, as shown in Figure 3(e). Compared to IEP, the fluorescence emission peaks of CIEP-x-y all exhibit different degrees of red shift, suggesting that the addition of different cations all induces stable cation-π interactions with the indole groups of IEP.[26]

Figure 3(f), obtained through crosslink density analysis via solid-state NMR, shows that after fitting, the IEP is 82.76, CIEP-Na-20 is 90.70, CIEP-Mg-20 is 89.35, and CIEP-K-20 is 89.91. The crosslink density of indole epoxy resins doped with cations is higher than that of IEP.

The above analysis demonstrates the presence of cation-π interactions in the prepared CIEP-x-y, allowing further investigation into the impact of different metal cation-induced cation-π interactions on the conjugated structure of indole epoxy resins through selective cation doping.

Mechanical Properties. The mechanical properties of IEP and CIEP were evaluated through uniaxial tensile testing. Figure 4(a) shows the stress-strain curve of IEP and CIEP-x-20. Figures 4(b), 4(c), and 4(d) display stress-strain curves for samples doped with different ions and varying cation proportions. CIEP-Mg-y (y = 5, 10) films were extremely brittle and could

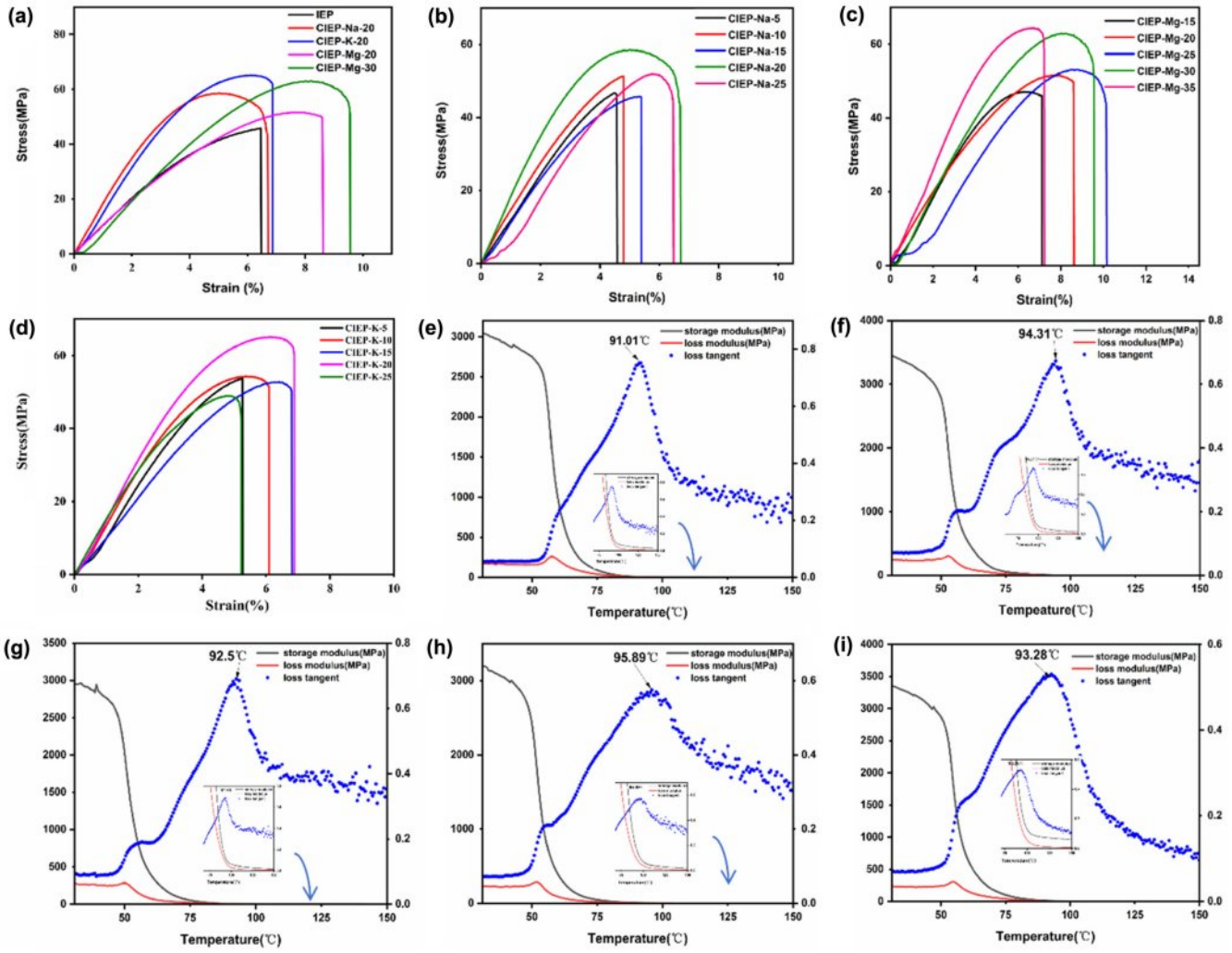

Figure 4. (a) IEP and CIEP-x-20 stress-strain curve diagram; (b) stress-strain curves of CIEP-Na-y (y = 5, 10, 15, 20, 25); (c) stress strain curves of CIEP-Mg-y (y = 15, 20, 25, 30, 35); (d) stress strain curves of CIEP-K-y (y = 5, 10, 15, 20, 25); (e) dynamic mechanical analysis of IEP; (f) dynamic mechanical analysis of CIEP-Na-20; (g) dynamic mechanical analysis of CIEP-Mg-20; (h) dynamic mechanical analysis of CIEP-Mg-30; (i) dynamic mechanical analysis of CIEP-K-20.

not undergo tensile testing. All cationically crosslinked samples were divided into five groups and tested with a proportion reduction of 5%. Table 2 presents maximum tensile strength and elongation at break for different cations and doping amounts. For CIEP-x-y (x = Na^+, K^+, Mg^{2+}), mechanical properties initially increase then decrease as cation content decreases.

When cations are doped into IEP from high to low content, the higher cation concentration leads to precipitation of cations in the form of inorganic salts during curing.[27] However, the presence of this inorganic salt leads to a reduction in tensile strength. As cation content decreases, cation-π interactions become dominant, increasing the internal forces within the polymer and thus enhancing tensile strength. However, when cation content drops below a critical value, the reduction in crosslinking points diminishes the reinforcing effect of cation-π interactions on the resin matrix, leading to decreased mechanical performance.

Based on data analysis, an internal analysis was conducted on epoxy resin matrices doped with different cations. Comparing the three ions at y = 20, the order of their strength is: K^+ > Na^+ > Mg^{2+} > IEP; the order of their elongation at break is: Mg^{2+} > Na^+ ≈ K^+ > IEP. However, among magnesium ion doping, the optimal performance is achieved with CIEP-30.

Compared to indole epoxy resin without added metal cations, the resin with cations shows higher strength and toughness, indicating cation incorporation influences its mechanical properties.[28] This effect primarily stems from cation addition,

Table 2. Maximum Tensile Strength and Maximum Elongation at Break Measured for Different Doping Levels of Cations

Sample	Tensile strength (MPa)	Fracture elongation rates (%)
CIEP-Na-5	46.65	4.49
CIEP-Na-10	51.22	4.75
CIEP-Na-15	45.63	5.38
CIEP-Na-20	58.45	6.70
CIEP-Na-25	51.75	6.44
CIEP-Mg-15	47.10	7.11
CIEP-Mg-20	51.49	8.59
CIEP-Mg-25	53.09	10.14
CIEP-Mg-30	62.88	9.52
CIEP-Mg-35	62.07	7.17
CIEP-K-5	53.56	5.21
CIEP-K-10	46.28	6.02
CIEP-K-15	54.18	6.08
CIEP-K-20	65.00	6.87
CIEP-K-25	48.87	4.90

which forms cation–π interactions that enhance and toughen the resin.

Among the three ions, for elements within the same group (K and Na), ionic radius is directly proportional to strength. For elements in the same period, both charge and radius vary, making neither ionic radius nor charge alone sufficient to compare strength or fracture elongation. However, the synergistic effect results in Mg^{2+} having lower strength but higher fracture elongation than Na^{+}. This experimental observation provides empirical support for the previous theoretical calculations. First, it demonstrates that in indole epoxy resin, the synergistic effect of ionic radius and charge in cation–π interactions influences the enhancement and toughening performance. Second, in theoretical simulations, this synergy affects the interaction energy, with Mg^{2+} exhibiting the lowest interaction energy; in mechanical testing, Mg^{2+} shows the lowest strength but the highest fracture elongation. Furthermore, the interaction energy order of the three cations is $K^{+} > Na^{+} > Mg^{2+}$, which is directly proportional to strength and inversely proportional to fracture elongation.

The polymer formed at y = 20 in Mg^{2+}-doped indole epoxy resin is not optimal for enhancing performance. The optimal doping level is at y = 30, where the strength reaches 62.88 MPa and the elongation at break reaches 9.52%. primary factor for this difference lies in the cation concentration: at y = 20, more cations are introduced into the indole epoxy resin compared to y = 30. This results in a denser cross-linked network structure, which restricts molecular chain mobility, thereby decreasing both tensile strength and elongation at break.

To further verify the impact on mechanical properties, dynamic mechanical analysis (DMA) tests were carried out on IEP and CIEP-x-y, as shown in Figures 4(e) to 4(i). Compared with IEP, the cation-added samples all show small peaks in the low-temperature region, indicating that the presence of cation-π interaction enables energy dissipation of indole epoxy resin at low temperatures. Moreover, the TG results of all CIEP-x-y samples are higher than those of IEP, which proves that the cation-π interaction improves the strength and toughness of indole epoxy resin.

Stress relaxation tests were also conducted on IEP and CIEP-x-y at 90 °C. As shown in Figure 5, the initial modulus of all CIEP-x-y samples was higher than that of IEP, and the relaxation rates of CIEP-x-y were all slower than that of IEP.

To further validate the mechanism by which cation-π interactions enhance the mechanical properties of IEP, scanning electron microscopy (SEM) was employed. Figure 6(a) to 6(d) displays the cross-sectional digital images of IEP and CIEP-x-y. The fracture surface of IEP is smooth, indicative of typical brittle fracture, whereas the fracture surface of CIEP-x-y is rough and exhibits curling, suggesting ductile fracture. This indicates that under external force, the cation-π interactions formed by IEP with added cations continuously dissipate energy to maintain sample integrity.[29] However, when the external force reaches its limit, these interactions cannot counteract the force, leading to crack formation and subsequent fracture.

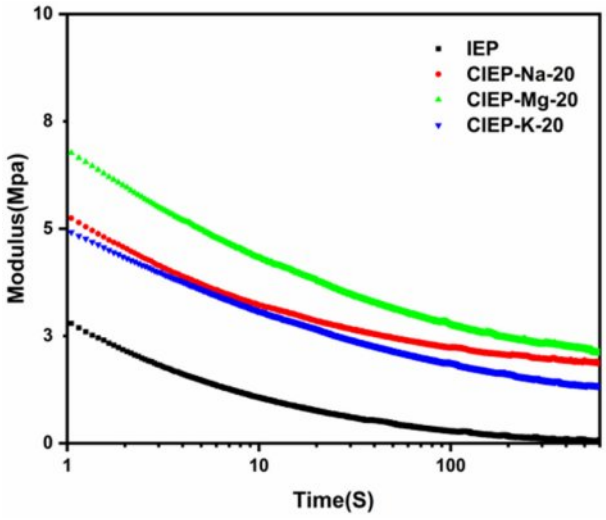

Figure 5. IEP and CIEP-x-y stress relaxation curves at 90 °C for 10 minutes.

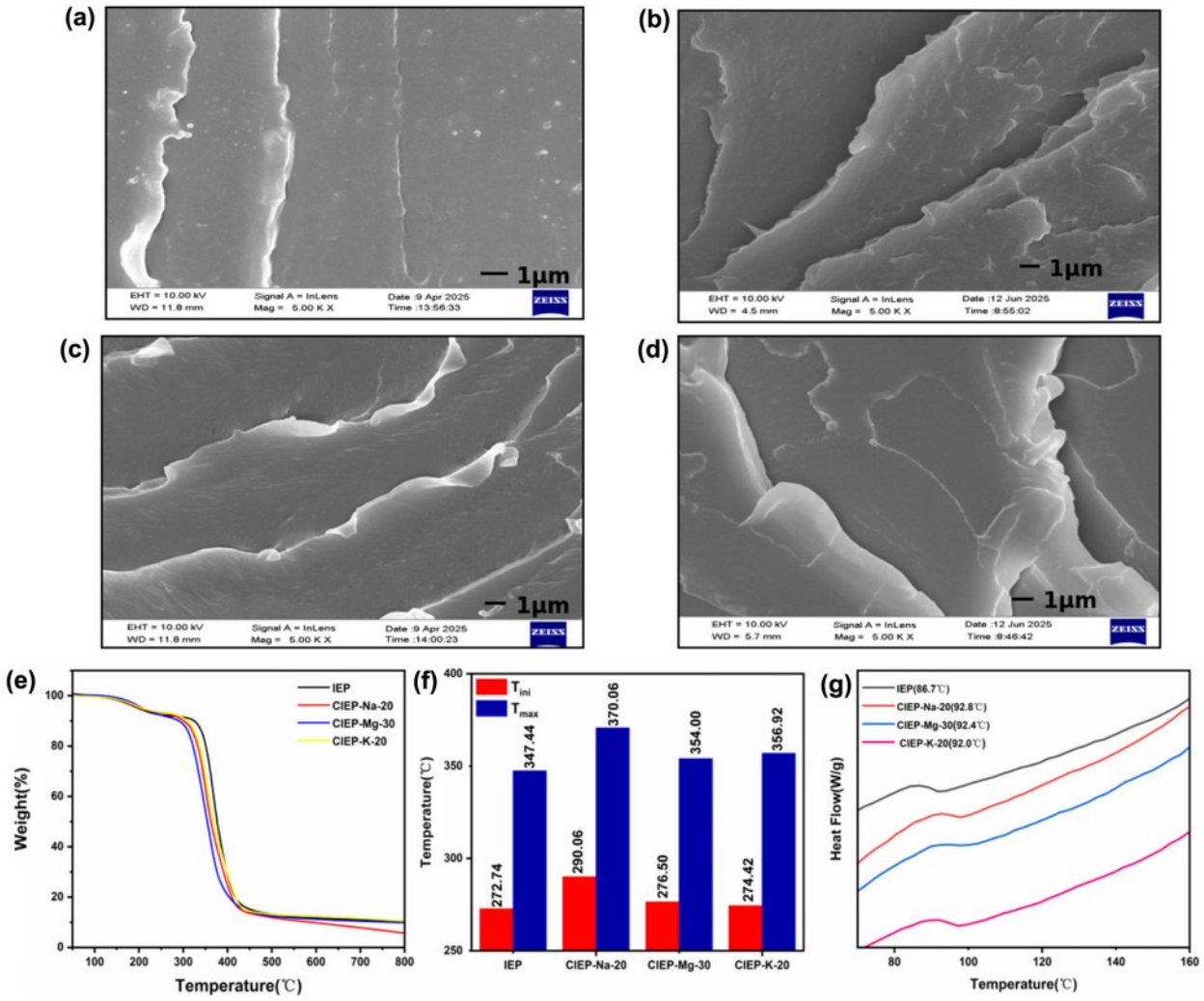

Figure 6. Sectional morphology of (a) IEP; (b) CIEP-Na-20; (c) CIEP-Mg-30; (d) CIEP-K-20; (e) TGA curves of IEP and CIEP-x-y; (f) Decomposition temperature Tini and maximum decomposition rate temperature Tmax curves of IEP and CIEP-x-y; (g) DSC curves of IEP and CIEP-x-y.

Thermal Decomposition Behavior. The cation-π interaction leads to differences in thermal properties between the formed CIEP-x-y and IEP. Figure 6(e) shows the thermogravimetric analysis (TGA) curves of IEP and CIEP-x-y. The weight loss within 100–200 °C can be attributed to the loss of residual DMF.[30] The decomposition of the formed polymer occurs in the range of 200–400 °C. As shown in Figure 6(f), the decomposition temperature and maximum decomposition temperature of CIEP-x-y are higher than those of IEP. Additionally, the initial decomposition temperature (T_{ini}) and maximum decomposition temperature (T_{max}) of CIEP-Mg-20 are lower than those of CIEP-x-y with the other three cations added.

The differential scanning calorimetry (DSC) curves are presented in Figure 6(g). The glass transition temperature (T_g) of IEP is 86.7 °C, while the T_g values increase to 92.8, 92.0 and 92.4 °C after the addition of Na^+, K^+ and Mg^{2+}, respectively. Compared to IEP, CIEP-x-y exhibits higher T_g values, which can primarily be attributed to the cation-π interactions.

Conclusions

Na^+, Mg^{2+}, and K^+ were successfully doped into indole epoxy resins, forming cation-π interactions confirmed by theoretical calculations and experimental tests. Mechanical property evaluations indicated that all three cations reinforced and toughened the resin, with varying degrees of enhancement. The strength order was $K^+ > Na^+ > Mg^{2+}$, which was proportional to interaction energy and ionic radius. Conversely, elongation at

break followed the order $Mg^{2+} > Na^{+} \approx K^{+}$, which was inversely proportional to interaction energy and ionic radius. Thus, microscopic interaction energy and ionic radius correlate with macroscopic mechanical properties, enabling rapid screening of raw materials for target properties and guiding material design and phase selection.

Acknowledgments: This work was financially supported by the Postgraduate Innovation Fund Project by Southwest University of Science and Technology (25ycx3001), Suining City's unveiling and leadership project (2025SNKBZ09). The authors acknowledge the technicians at Shenzhen HUASUAN Technology Co., Ltd. for assistance with theoretical calculations.

Conflict of Interest: The authors declare that there is no conflict of interest.

Supporting Information: Theoretical calculations and experimental proof of Cation-π Interactions Formed by Different Metal Cations (PDF). The materials are available *via* the Internet at http://journal.polymer-korea.or.kr.

References

1. Kumar, N.; Gaur, A. S.; Sastry, G. N. A Perspective on the Nature of Cation–π Interactions. *J. Chem. Sci*. **2021**, 133, 97.
2. Zhao, G.; Zhu, H. Cation–π Interactions in Graphene-containing Systems for Water Treatment and Beyond. *Adv. Mater.* **2020**, 32, 1905756.
3. Dougherty, D. A. The Cation–π Interaction in Chemistry and Biology. *Chem. Rev.* **2025**, 125, 2793-2808.
4. Kennedy, C. R.; Lin, S.; Jacobsen, E. N. The Cation–π Interaction in Small-molecule Catalysis. *Angew. Chem. Int. Ed.* **2016**, 55, 12596-12624.
5. Mu, B.; Yang, Z.; Liang, Z.; Xue, R.; Bu, L.; Zhang, H.; Chi, L.; Yan, H.; Tian, W. Conductive Two-dimensional Supramolecular Polymers *via* Cation–π Driven Self-aligned Aromatic Brick-like Stacking. *CCS Chem*. **2025**, 7, 807-818.
6. Luo, J.; Chen, K.; Yin, P.; Li, T.; Wan, G.; Ye, S.; Bi, X.; Pang, Y.; Wei, Y. Effect of Cation–π Interaction on Macroionic Self-assembly. *Angew. Chem*. **2018**, 130, 4131-4136.
7. Jiang, G.; Yu, J.; Wang, J.; Tang, B. Z. Ion–π Interactions for Constructing Organic Luminescent Materials: Special Issue: Emerging Investigators. *Aggregate*, **2022**, 3, e285.
8. Li, Q.; Li, W.; Liu, Z.; Zheng, S.; Wang, X.; Xiong, J.; Yan, F. Poly(ionic liquid) Double-network Elastomers with High-impact Resistance Enhanced by Cation–π Interactions. *Adv. Mater.* **2024**, 36, 2311214.
9. Chen, S.; Li, Z.; Zhang, C.; Wu, X.; Wang, Q.; Chen, W.; Shi, J. Yuan, D. Cation–π Interaction Trigger Supramolecular Hydrogelation of Peptide Amphiphiles. *Small*, **2023**, 19, 2301063.
10. Huang, Z.; Zhao, K.; Wei, S.; Hao, Y.; Yu, Q.; Hao, J.; Cui, J.; Zhang, P. Rapid Formation of Antifouling Coatings *via* Cation–π Interactions. *Polym. Chem*. **2024**, 15, 4465-4473.
11. He, M.; Li, J.; Xu, J.; Wu, L.; Li, N.; Zhang, S. Dynamic Recyclable High-performance Epoxy Resins *via* Triazolinedione–indole Click Reaction and Cation–π Interaction Synergistic Crosslinking. *Polymers*, **2024**, 16, 1900.
12. Zhou, T.; Wang, N.; Gao, Y.; Li, X. Cation–π Interactions in Polymer Science: From Fundamental Insights to Material Applications. *Polym. Chem*. **2025**, 16, 2058-2074.
13. Guan, X-f.; Liao, C.; Yang, L.; Chang, G-j. Indole-based High-performance Polymeric Materials with Enhanced Mechanical and Thermal Properties *via* Cation–π Interaction. *High Perform. Polym*. **2020**, 32, 662-668.
14. Tang, Q.; Zhu, F.; Li, Y.; Peng, Q.; Kang, M.; Kang, T. Engineering Tunable Light Color in High-performance Rare Earth Fluorescent Polymers *via* Cation–π Interactions. *ACS Appl. Polym. Mater.* **2024**, 7, 529-537.
15. Zhuo, L.; He, L.; Wang, Y.; Gou, P.; Wang, X.; Hu, G.; Xie, F. Highly Efficient Thermal Insulation Polyimide Foams Enhanced by Cation–π Interactions. *J. Mater. Sci*. **2024**, 59, 20092-20106.
16. Zhao, S.; Sun, L.; Liu, Y.; Gao, C.; Ding, L.; Kan, Z.; Liu, Y. Cation-indole Supramolecular Interaction Constructed Novel Silicone Anti-fouling Materials. *Chem. Eng. J*. **2025**, 505, 159423.
17. Wei, P.; Zhao, W.; Han, S. Research on Impact Resistance Performance of Pbo Fiber Reinforced Polyurea Composites. *Coat. Prot.* **2025**, 46, 49-56.
18. Lu, T.; Chen, Q. Interaction Region Indicator: A Simple Real Space Function Clearly Revealing Both Chemical Bonds and Weak Interactions. *Chem. Methods*, **2021**, 1, 231-239.
19. Lu, T.; Chen, F. Multiwfn: A Multifunctional Wavefunction Analyzer. *J. Comput. Chem*. **2012**, 33, 580-592.
20. Lu, T. Visualization Analysis of Covalent and Noncovalent Interactions in Real Space. *Angew. Chem. Int. Ed.*, **2025**, 64, e202504895.
21. Lu, T.; Chen, Q. A Simple Method of Identifying π Orbitals for Non-planar Systems and a Protocol of Studying π Electronic Structure. *Theor. Chem. Acc*. **2020**, 139, 25.
22. Just, G. H.; Lefebvre, C.; Rajamani, A.; Khartabil, H.; Pilme, J.; Hénon, É. A Visualizable and Widely Applicable Steric Repulsion Descriptor for Guiding Experimental Chemistry. *Chem. Sci*. **2026**, 17, 5394-5403.
23. Chang, G.; Yang, L.; Yang, J.; Stoykovich, M. P.; Deng, X.; Cui, J.; Wang, D. High-performance pH-switchable Supramolecular Thermosets *via* Cation–π Interactions. *Adv. Mater*., **2018**, 30, 1704234.
24. Tang, Q.; Zhu, F.; Li, Y.; Yin, S.; Xu, Y.; Yan, H.; Kang, M.; Chang, G. Demonstration of π–π Stacking at Interfaces: Synthesis of an Indole-Modified Monodisperse Silica Microsphere SiO_2@IN. *Langmuir*, **2024**, 40, 8685-8693.
25. Yorita, H.; Otomo, K.; Hiramatsu, H.; Toyama, A.; Miura, T.; Takeuchi, H. Evidence for the Cation–π Interaction Between Cu^{2+}

and Tryptophan. *J. Am. Chem. Soc*. **2008**, 130, 15266-15267.
26. Li, Y.; Du, M.; Yang, L.; Bao, Y.; Xu, Y.; Yin, Q.; Lan, Y.; Chang, G. Hydrophilic Domains Compose of Interlocking Cation–π Blocks for Constructing Hard Actuator with Robustness and Rapid Humidity Responsiveness. *Chem. Eng. J.* **2021**, 414, 128820.
27. Yang, L.; Li, Y.; Du, M.; He, Y.; Lan, Y.; Yin, Q.; Zhu, F.; Chang, G. Force-reversible and Energetic Indole-Mg-Indole Cation–π Interaction for Designing Toughened and Multifunctional High-performance Thermosets. *Adv. Funct. Mater.* **2022**, 32, 2111021.
28. Li, Y.; Zhu, F.; Tang, Q.; Zhang, J.; Peng, Q.; Kang, M. Preparation of High-performance Red Fluorescent Epoxy Resin Films Guided by Rare Earth Europium. *Mater. Sci. Technol.* **2025**, 42, 576-586.
29. Tang, Q.; Li, H.; Yin, S.; Peng, Q.; Kang, M.; Kang, T.; Liu, J.; Wang, H.; Chang, G. Synergistic Strengthening and Toughening of Epoxy Composites via Li^{+}-π Interaction Induced Microsphere Rolling Mechanism: Rotational Stability and Wide-Range Effect. *Adv. Funct. Mater.* **2026**, 13, e09971.
30. Wu, Y.; Breeze, M. I.; Clarkson, G. J.; Millange, F.; O'Hare, D.; Walton, R. I. Exchange of Coordinated Solvent During Crystallization of a Metal–Organic Framework Observed by In Situ High-Energy X-ray Diffraction. *Ang. Chem.* **2016**, 128, 5076-5080.